SUPPLEMENTARY INFORMATION

Large-area sputtered 2H-MoS_2 thin films for spin and orbital charge conversion

A. S. Vieira,[1] G. R. Gallo,[1] E. Santos,[2] G. Rodrigues-Junior,[1] R. Cardias,[3] T. G. Rappoport,[3,4] L. G. Moura,[1] R. O. Cunha,[1] A. Azevedo,[2] J. B. S. Mendes[1*]

[1]*Departamento de Física, Universidade Federal de Viçosa, 36570-900 Viçosa, MG, Brasil*
[2]*Departamento de Física, Universidade Federal de Pernambuco, 50670-901 Recife, PE, Brasil*
[3]*Centro Brasileiro de Pesquisas Físicas (CBPF), 22290-180 Rio de Janeiro, RJ, Brasil*
[4]*International Iberian Nanotechnology Laboratory (INL), Av. Mestre José Veiga, 4715-330 Braga, Portugal*

Morphological, structural, electrical and chemical analysis of sputtered MoS_2 thin films after annealing treatment

S1. X-ray reflectivity analysis of MoS_2 samples

X-ray reflectivity (XRR) measurements were carried out to investigate the structural properties of the MoS_2 samples, including thickness, density, and surface/interface roughness. The data were acquired using a Bruker D8 Discover diffractometer equipped with a monochromatic Cu Kα radiation source. XRR pattern of nominal 50 nm-thick MoS_2 samples as a function of different annealing temperatures are plotted in Fig. S1(a). A well-defined oscillatory profile is observed for samples annealed above 400 °C, indicating a sharp interface between the sputtered MoS_2 and the SiO_2 substrate. Nevertheless, the untreated sample does not exhibit such features, evidencing its low structural quality. Furthermore, Fig. S1(b–e) highlights the XRR patterns of the samples annealed between 500 °C and 800 °C. The experimental data are shown as black dots, while the red solid lines represent the fits obtained through simulations using the Parratt formalism. These fits provide valuable information about the film density, thickness, and both surface and interface roughness of the MoS_2 films. Table S1 summarizes the values extracted from the fittings. As can be seen, sputtered MoS_2 films annealed at high temperatures exhibit mass density values ranging from 4.80 g/cm^3 to 5.22 g/cm^3, deviating by only ~5% from the theoretical density of bulk crystalline MoS_2

(5.06 g/cm^3) [1]. This small variation may be attributed to crystalline imperfections such as strain, grain boundaries, and other types of disorder. Additionally, the surface roughness values obtained by XRR analysis are consistent with the AFM measurements, both reporting values below 1 nm. Moreover, the interface roughness between the MoS_2 films and the SiO_2 substrate also remains low, ranging from 0.40 nm to 0.55 nm. This indicates stable interface quality and suggests that no significant interdiffusion occurred during high-temperature annealing treatments.

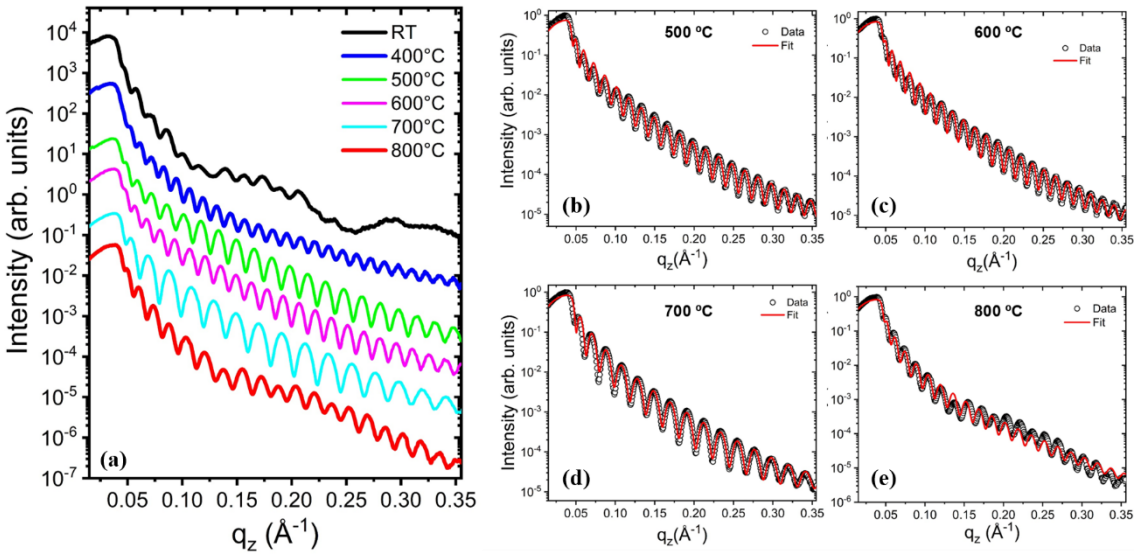

Figure S1. (a) XRR profiles of 50nm MoS_2 samples as a function of thermal annealing at different temperatures. (b-d) Experimental XRR data (black dots) for samples annealed at higher temperatures. The red solid lines are the corresponding fits obtained using the Parratt formalism.

Table S1: Structural properties of annealed 50 nm-thick MoS_2 films obtained from XRR fitting.

Temperature (ºC)	Density (g/cm^3)	Surface Roughness (nm)	Interface Roughness (nm)
500 ºC	4.87	0.29	0.50
600 ºC	5.22	0.28	0.40
700 ºC	4.87	0.11	0.48
800 ºC	4.80	0.36	0.55

S2. XRD measurements of MoS_2 films

The crystalline structure of sputtered MoS_2 films was analyzed by X-ray diffraction (XRD) using the same diffractometer described above. Fig. S2(a) depicts a typical symmetrical 2theta-omega XRD pattern of 100 nm-thick MoS_2 sputtered on SiO_2, showing an intense peak at $2\theta \cong 69.1°$ corresponding to the (400) plane of Si from the substrate, which was attenuated using a Ni filter to enhance the visibility of the MoS_2 diffraction signal. A diffraction peak at $2\theta \approx 13.9°$ is clearly visible and can be indexed to the (002) plane of the 2H-MoS_2 phase, with its position being close to the value typically reported in the literature ($2\theta \approx 14.2°$). The observation of only the (002) reflection from MoS_2, without other polycrystalline contributions, indicates a strong preferential orientation with the c-axis perpendicular to the substrate surface. This texture is characteristic of polycrystalline layered transition metal dichalcogenide thin films grown under conditions that promote van der Waals stacking along the out-of-plane direction. For comparison, Fig. S2(b) shows the XRD pattern of the bare Si/SiO_2 substrate.

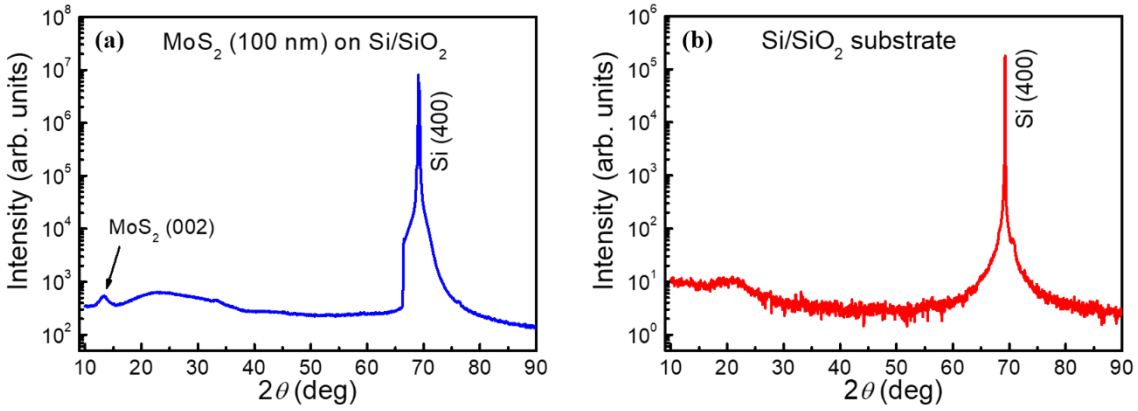

Figure S2. (a) XRD pattern of a 100 nm-thick MoS_2 film deposited by sputtering on a Si/SiO_2 substrate. (b) XRD pattern of the bare Si/SiO_2 (100) substrate.

S3. HRTEM images of MoS_2 films

The morphological and structural characteristics of cross-sectional sputtered MoS_2 films were investigated by high-resolution transmission electron microscopy (HRTEM) performed with a monochromated FEI Titan Cubed Themis field emission electron microscope with accelerating voltage at 300 keV. All image processing, including pixel intensity filtering, digital zoom, and contrast enhancement, was performed using ImageJ software. Fig. S3(a) shows a cross-sectional STEM image acquired using a bright-field (BF) detector for the 5 nm-thick MoS_2 sample annealed at

600 °C. A clear polycrystalline texture can be observed throughout the film. The inset boxes highlight selected regions of the image to emphasize specific structural features of the MoS_2 lattice at different positions. Fig. S3(b–d) shows digital zooms of regions 1 (blue box), 2 (red box), and 3 (green box), respectively, highlighting details of the atomic arrangement and lattice orientation. The corresponding processed images are presented in Fig. S3(e–g), obtained by applying a minimum-intensity pixel filter to panels (b–d). These filtered images enhance the visibility of the hexagonal lattice structure, clearly revealing the characteristic atomic configuration of the 2H-MoS_2 phase in the selected regions. These observations provide additional evidence of the crystalline quality of the sample. Additionally, Fig. S3(d) and S3(g) show a subtle change in lattice orientation, delimited by black and white dashed lines, which can be associated with a grain boundary domain.

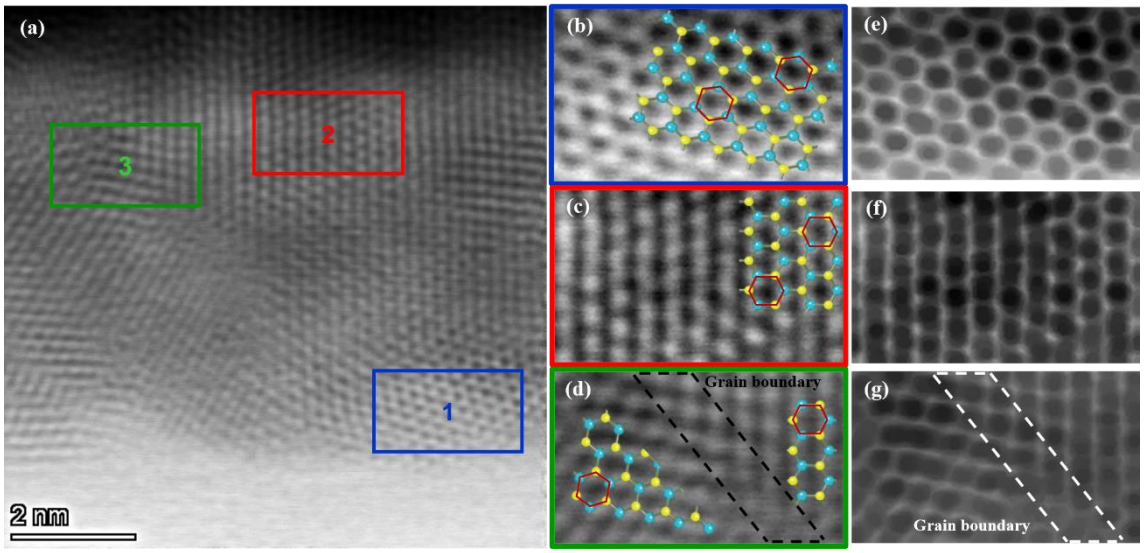

Figure S3. (a) Cross-sectional STEM-BF image of a 5 nm MoS_2 film. Each solid box inset highlights a region of the sample with a different crystallographic orientation, evidencing the polycrystalline nature of the film. (b)–(d) Magnified views of the regions marked as 1 (blue), 2 (red), and 3 (green) in panel (a), respectively. (e)–(g) Corresponding images of panels (b)–(d) after applying a minimum-intensity pixel filter, revealing the hexagonal lattice structure in the selected regions.

S4. Cross-sectional images of MoS_2 samples

Figure S4(a) shows a cross-sectional image of a 5 nm-thick MoS_2 film, annealed at 600 ºC, deposited on a SiO_2 substrate, and covered with a 6 nm Pt-sputtered cap-layer. The red dashed lines illustrate the approximate stacking of MoS_2 layers, with an interlayer distance of approximately 0.65 nm, consistent with the reported interlayer spacing for

2H-MoS_2 in the literature [2]. It is important to note that this representation is schematic and not intended to represent atomic-scale accuracy. Fig. S4(b) displays a high-magnified STEM-BF image of the same sample, where it is possible to observe the polycrystalline nature of both the MoS_2 film and the Pt cap-layer. This characteristic is expected and commonly observed in sputtered samples. The red solid box inset in Fig. S4(b) depicts a zoomed image highlighting the interface between the MoS_2 film and the sputtered Pt layer, suggesting good atomic-level affinity between these two materials, which is crucial for spintronic applications.

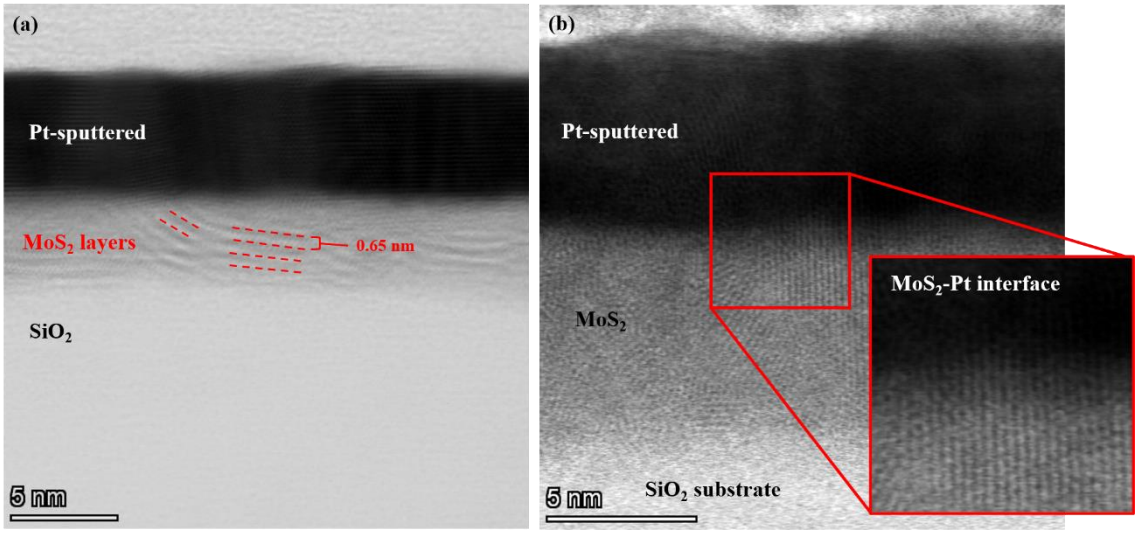

Figure S4. (a) Cross-sectional STEM-BF image of a 5 nm MoS_2 film, showing well-defined regions corresponding to the substrate, the MoS_2 layer, and the Pt top layer. Red dashed lines illustrate a schematic representation of the approximate stacking of MoS_2 layers. (b) STEM-BF image of the MoS_2/Pt interface. The red solid box highlights with more detail the interface between MoS_2 and Pt.

S5. EDX analysis of MoS_2 samples

To investigate the chemical composition and elemental distribution of the sputtered MoS_2 film, atomic-resolution energy-dispersive X-ray spectroscopy (EDX) was employed simultaneously with TEM images acquisition. Fig. S5(a) shows a typical cross-sectional STEM image of the 50 nm-thick MoS_2 sample, revealing a well-defined sputtered film deposited on the SiO_2 substrate. The carbon layer on top results from the protective capping layer deposited during the lamella preparation by focused ion beam (FIB). Figs. S5(b–f) display the elemental maps of the analyzed region, corresponding to: (b) oxygen (O, orange), (c) sulfur (S, green), (d) silicon (Si, cyan), (e) molybdenum (Mo, red), and (f) carbon (C, blue). A uniform distribution of S and Mo is observed throughout

the MoS_2 film, especially near the SiO_2/MoS_2 interface. This result indicates that the post-deposition annealing did not lead to interfacial diffusion or elemental segregation, which is consistent with the XRR results discussed before. Fig. S5(g) presents an EDX elemental map combining all the signals shown in Fig. S5(b–f), while Fig. S5(h) shows the corresponding EDX depth profile of O, Si, S, Mo, and C elements, measured across the region delimited by the black box inset in Fig. S5(g). The elemental distribution is homogeneous and well defined, with Mo and S signals oscillating around consistent intensity levels, as mentioned before. This observation reinforces the homogeneous composition of the MoS_2 film and further supports the absence of elemental segregation or diffusion at the film and the substrate interface. The strong peaks corresponding to Mo and S confirm their presence in the film, despite the proximity of their characteristic X-ray energies. Two additional intense peaks are associated with the substrate composition, specifically silicon (Si) and oxygen (O). Further signals include copper (Cu), originating from the TEM grid; gallium (Ga), resulting from residual implantation during the FIB milling process; and platinum (Pt), from the protective layer deposited during sample preparation.

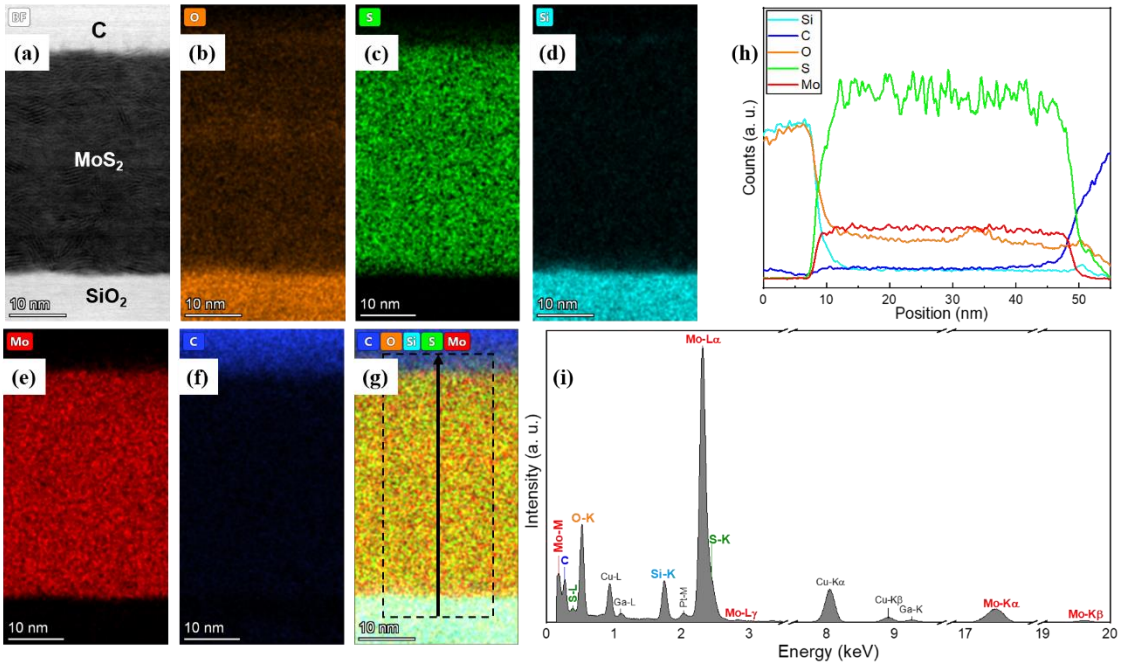

Figure S5. (a) Cross-sectional STEM-BF image and (b-f) corresponding EDS elemental maps of a 50 nm MoS_2 film deposited on SiO_2 substrate. The carbon signal is due to a protective layer by FIB lamella preparation. Elemental distributions are represented as: oxygen (O, orange), sulfur (S, green), silicon (Si, cyan), molybdenum (Mo, red), and carbon (C, blue). (g) Integrated EDS map combining the elemental signals, and (h) EDS

line scan showing the intensity variation of O, Si, S, Mo, and C across the region indicated by the black box in (g). (i) EDS spectra collected from the entire imaged area.

S6. AFM measurements of MoS_2 films

To investigate the surface morphology of sputtered MoS_2 thin films after thermal annealing, we performed AFM measurements using a NanoSurf FLEX AFM operating in tapping mode. AFM images of the 50 nm MoS_2 sample without annealing (0 °C, used as a reference) and of samples annealed at higher temperatures (>400 °C) are shown in Fig. S6(a–e). A clear granular morphology is observed, which is further highlighted in the corresponding 3D representations shown below each image. The granular surface morphology, which is typical for films grown by the sputtering method, remains qualitatively similar across all annealing conditions. However, subtle variations in grain size and surface roughness can be observed as a function of annealing temperature. Figure S6(f) shows the root mean square (RMS) roughness values as a function of annealing temperature (excluding the reference sample at 0 °C), obtained from Gwyddion software analysis over the entire image area. The results indicate a progressive decrease in roughness up to the sample annealed at 600 °C, followed by a slight increase for the sample annealed at 700 °C and 800 ºC. Qualitative observations combined with roughness measurements of the AFM images indicate that the samples exhibit homogeneous and uniform MoS_2 coverage over a large area, with RMS roughness values below 1 nm, as shown in Table 2. These results are further supported by XRR measurements.

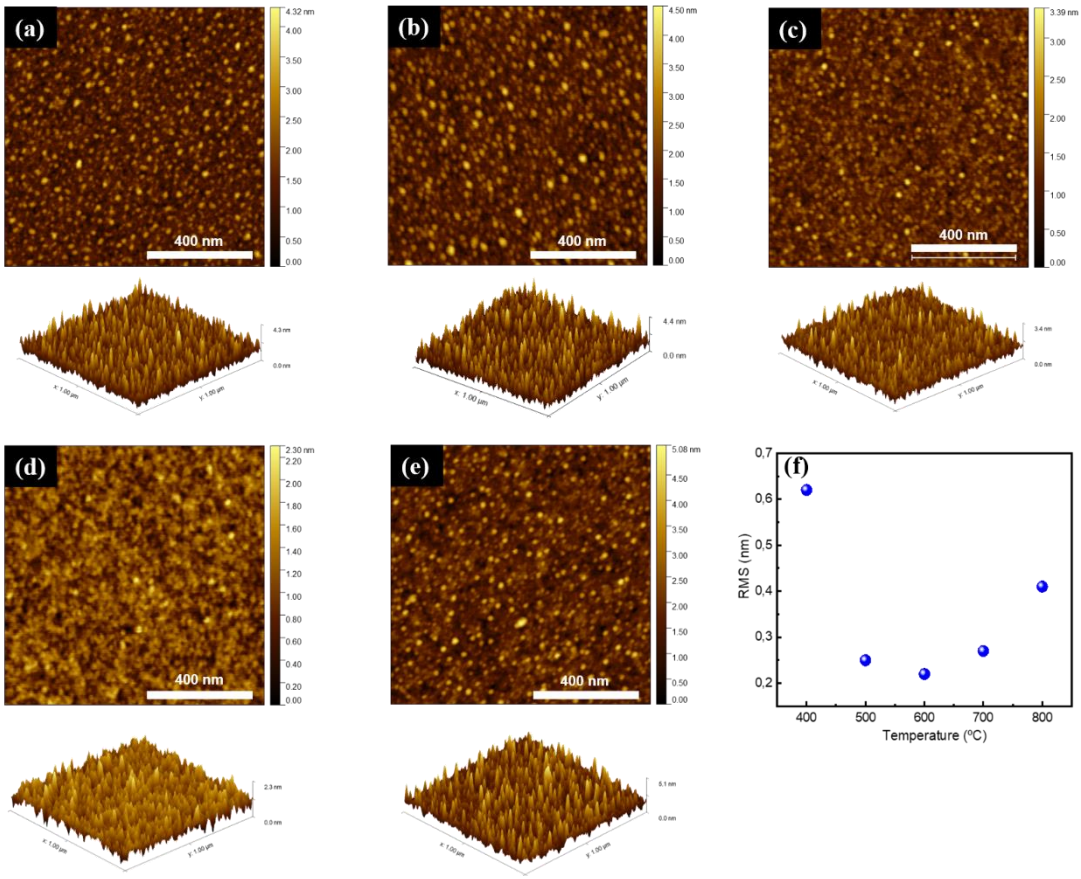

Figure S6. AFM images (1 μm × 1μm) of 50 nm MoS_2 films deposited on Si/SiO_2 substrates after thermal annealing at different temperatures: (a) 0 ºC as a reference sample, (b) 400 ºC, (c) 500 ºC, (d) 600 ºC, and (e) 800 ºC. The corresponding 3D surface topographies are shown below each 2D image. (f) RMS roughness values as a function of annealing temperature excluding the reference sample (0 ºC).

Table 2: RMS roughness values.

Temperature (ºC)	RMS Rough. (nm)
0	0.36
400	0.62
500	0.25
600	0.22
700	0.27
800	0.41

S7. FESEM images of 50 nm-thick MoS_2 samples

The morphology of the MoS_2 samples was also examined using scanning electron microscopy (SEM), performed on a Tescan Mira microscope equipped with a Schottky field-emission gun (FESEM). All images were acquired under identical conditions of scale, magnification, and accelerating voltage, with only minor adjustments in focus and contrast to enhance visualization. For all samples shown in Fig. S7 (0 °C and 400–800 °C), a smooth surface with no apparent structural irregularities is observed. Granular features or grain size distribution are barely discernible, qualitatively supporting the homogeneous and uniform deposition of MoS_2, as well as the low surface roughness values previously reported by AFM measurements.

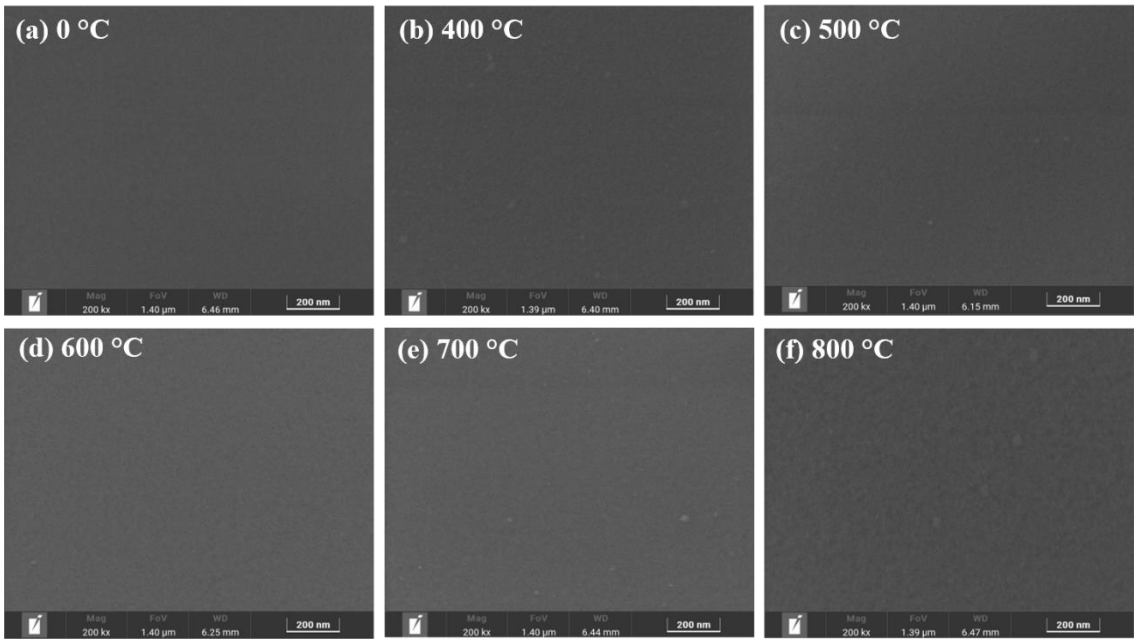

Figure S7. SEM images of 50 nm MoS_2 films deposited on SiO_2/Si substrates following thermal annealing at various temperatures: (a) 0 ºC, (b) 400 ºC, (c) 500 ºC, (d) 600 ºC, (e) 700 ºC, and (f) 800 ºC.

S8. I-V curve of MoS_2 films and Ti/Au electric contact

For the spin pumping measurements, a 20 nm thick Py (Permalloy, $Ni_{81}Fe_{19}$) film was sputter-deposited in a high vacuum chamber with a base pressure of 2.0×10^{-7} torr onto MoS_2 film, forming an island at the center of sample, as shown in the schematic of Fig. S8(a). To ensure ohmic contact in the MoS_2 layer, Ti (5 nm)/Au (50 nm) strips were deposited by sputtering on the ends of the sample. Two thin copper electrodes were fixed to the Ti/Au strips by means of silver paint and connected to the nanovoltmeter. These electrical contacts are not in contact with the Py film to prevent current shunting.

Therefore, Fig. S8(b) shows the I-V curve of one typical device used in this work exhibiting the ohmic electrical contact between the metal and the semiconductor.

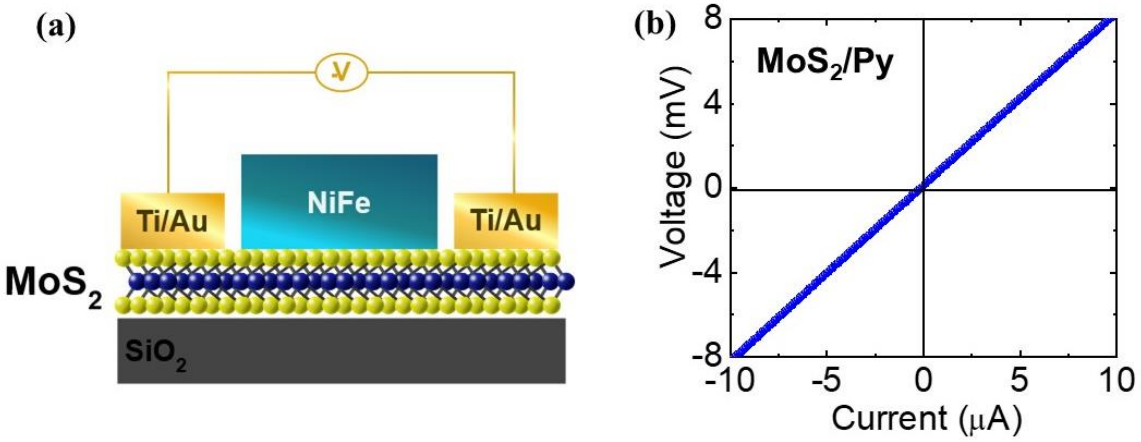

Figure S8. (a) Schematic representation of the sample for spin pumping measurements. (b) Typical IxV curve confirming the Ohmic behavior of the MoS_2 film and Ti/Au electrical contacts.

References

[1] Traill, R. J. *A Rhombohedral Polytype of Molybdenite*. The Canadian Mineralogist 7 (3), 524–526 (1963).

[2] Yi, M. & Zhang, C. The synthesis of two-dimensional MoS2 nanosheets with enhanced tribological properties as oil additives. *RSC Adv* 8, 9564–9573 (2018).